THE EFFECT OF THE PHYSICAL PARAMETERIZATION SCHEMES IN WRF-ARW ON THE QUALITY OF THE PREDICTION OF HEAVY RAINS THAT CAUSE FLOODING APPLICATION ON EASTERN ALGERIA

GASSI K.A.A.[1]*, SAOUDI H. [2]

[1] State engineer in meteorology, Forecasting and aeronautical assistance section, meteorological department of eastern region, Algerian national meteorological office (ONM), Constantine, Algeria

[2] Doctoral student, Laboratory: city, regions and territorial governance (LVRGT), faculty of earth sciences, geography and territorial planning (FSTGAT), university of sciences and technologies Houari Boumedienne (USTHB) Algiers, Algeria

(*) khaledgassi0@gmail.com

ABSTRACT

This study examines for the first time the impacts of the different physical parameterization schemes in the Weather Research and Forecasting (WRF-ARW) model on the quality of heavy rain prediction during the transitional season in eastern Algeria. Various physical model configurations are examined and verified by considering 144 numerical experiences using different combinations of cumulus and microphysical schemes compared to rain records of a network of thirty specialized meteorological stations for the period from August 1 until the last of October 2022. The most reliable forecasts have been obtained from the Kain-Fritsch cumulus scheme (KF). However, the impact of microphysical schemes was not truly identified in our study cases.

Keywords: WRF-ARW, Heavy rains, Transitional season, Eastern Algeria, Cumulus, Microphysics

INTRODUCTION

Algeria is a country of middle latitudes in the Northern Hemisphere. In eastern Algeria, there are generally four seasons in the year. One rainy season, one dry season and two transition seasons alternate. The transitional seasons cover the months of March through June and August through early October (Zeggane et al., 2021). They are recognized by the torrential rains associated with rainy thunderstorms, resulting from a contribution of

moisture to the middle layers of the troposphere with natural convection during the sun's day, and in a couple of hours, there will be a multicellular formation in some super cellular systems. The result is heavy rain in the shape of a shower in a very short time that leads to flash floods (Charles, 1993; Hafnaoui et al., 2022; Pang and Tan, 2023; Bong et al., 2023). Examples include the flooding of Skikda and Jijel on 2 September 2019 and the flooding of 5 October 2022 in Bordj Bou Arreridj.

Fig. 1 shows the number of rainy days classified by intensity for Constantine's wilaya over 30 years. February, April, September and November are known for torrential rains. April and September are part of the transition period, and the rest is related to the traditional winter system.
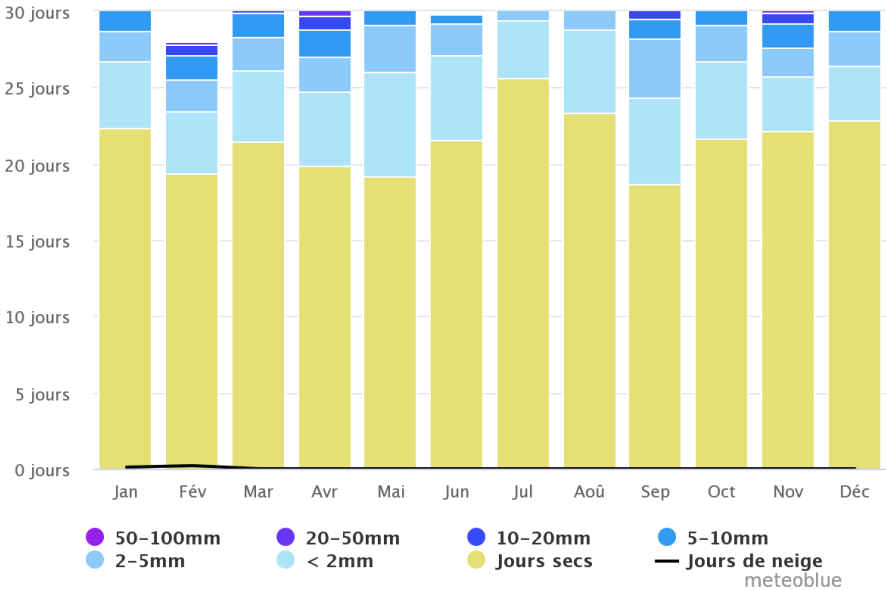
Figure 1: Diagram of the number of rainy days classified by intensity for the wilaya of Constantine

Accurate prediction of floods requires reliable estimates of extreme rainfall events (Cherki, 2019; Nassa et al., 2021). Modeling heavy rainfall has been challenging due to multiscale interactions and model configurations. Different numerical models are used for operational forecasting, and limited area models are preferred for predicting small-scale phenomena such as storm rain (Roderick, 2021). The Weather Research and Forecasting-Advanced Research Model (WRF-ARW) is a mesoscale model designed to improve predictions of these phenomena. This model consists of dynamic solvers with physical parameterizations of small-scale phenomena in the form of a numerical scheme, giving its physical part, as shown in Fig. 2 (Alexander et al., 2018).
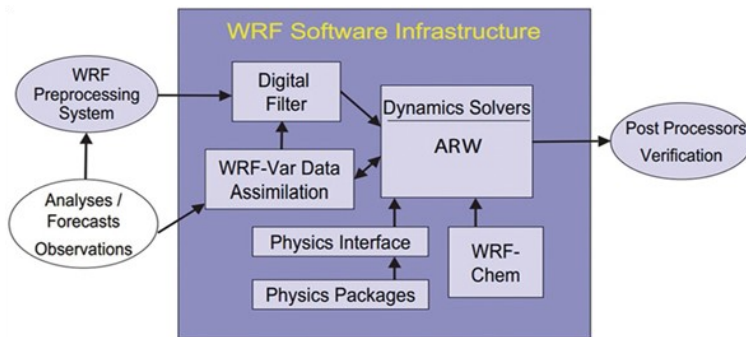
Figure 2: WRF-ARW software infrastructure.

Fig. 2 shows the WRF-ARW software infrastructure, which consists of three components:

- A preprocessing system consists of observed data, draft forecasts and analyses.

- A calculation core consists of a filter fed by the assimilated data, running in a dynamics solver that uses the physical interfaces and the packages and the chemical packages.

- And a viewing and control station.

There are five types of parameterization schemes used in numerical weather prediction models: radiation, land surface model, microphysics (MP), cumulus (CP) and planetary boundary layer (PBL). These schemes play a dominant role in the initiation and development of weather systems such as convective rainfall events and storms, land–sea breezes, thermal boundaries and mountain valley circulations. The skill of these parameterization schemes varies with specific events and regimes (Triphonia et al., 2018).

In the WRF model, users have the flexibility to select from different physical parameterizations. However, this choice depends on the location of interest, type of application, spatial and temporal resolutions or the type of prevailing weather phenomena of the region.

To improve the quality of WRF-ARW predictions, several research projects have been carried out worldwide. Each search aims to find the best configuration for a region during a given event or period. Recent research has detected that selecting the right combination of physical schemes, especially cumulus and microphysics schemes, is essential for better performance of the model's rainfall prediction, which eventually improves the forecast skill of the model (Skamarock et al., 2008). A study of sensitivity to cumulus and microphysical patterns was addressed by (Yandy G et al., 2015), and combinations of cumulus and microphysical patterns were tested to select the combination that most accurately represented a heavy precipitation event over Cuba. In another study (Yasmin Kaore et al., 2022), various combinations of seven microphysics, three cumuls and three planetary boundary layers were assessed. to simulate hourly precipitation during an

unusual extreme precipitation event that occurred in the city of El Salvador. Relevant studies were conducted primarily at mid-latitudes (Hiren et al., 2018), (Julia et al., 2019) and (Tien et al., 2019). Few studies have been conducted near Algeria (Jorge et al., 2022). However, no study has been done on Algeria.

In this context, this study uses the WRF model to investigate the impact of different physical parameterizations and determine the best schemes for the simulation of extreme rain events in eastern Algeria by considering a representative event that occurred during the transitional season from August to October 2022. In addition, systems are more common in isolated mode during this period.

METHODOLOGY

Study Area

The study took place in eastern Algeria between latitudes 33°42'45" and 37°7°10" to the north and 4 16'51" and 8°41'45" to the east. It is composed mainly of 16 wilayas, containing a well-placed and effective weather observation network (Fig. 3).
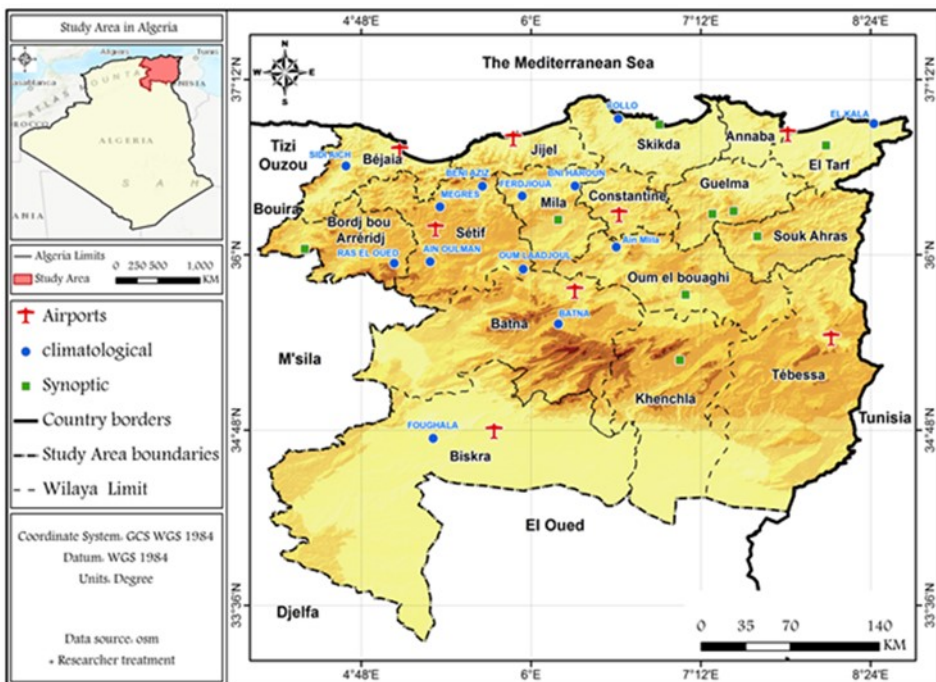
Figure 3: Study area and the observation network used.

126

Data collected

To collect the situations, we rely on the total precipitation of 24 hours recorded each day from 6 am until 6 am. To validate the existence of thunderclouds and confirm that the observation comes from rainstorm systems, we examined each station's METAR (Meteorological Aerodrome Report) messages plus corresponding satellite images by the company that owns the EUMETSAT weather satellites, particularly for climatological stations. The meteorological observation network data of the eastern region, under the approval of the World Meteorological Organization, will be used as databases. The observation network consists of 13 automatic stations for climatological use, 8 professional airport stations and 9 synoptic stations, as shown in Fig. 3.

Model Description

This study used the recently released version of the Weather Research and Forecasting model with the ARW dynamical core (WRF-ARW model; version 4.4.2) to feed the Global Forecasting System (GFS) data, with a horizontal resolution of 3 km and a vertical resolution of 45 levels over eastern Algeria, utilizing multiple physical combinations. The complete configuration of the model is shown in Table 1.

Table 1: The configuration of the WRF-ARW model used.

Model		WRF-ARW
Cycle		V4.4.2
Coupling frequency		1 H
Coupling model		GFS
Horizontal Resolution		3 km
Vertical Resolution		45 levels
Time step		60 s
Domain	Longitude	4°10'E--8°50'E
	Latitude	33°50'N--37°8'N
Grid		157*156
The basics of forecasting		00 H
Scope		48 H

Experimental Design

Convective parameterization continues to be one of the most challenging aspects of numerical modeling of the atmosphere, especially for numerical weather prediction and global climate prediction. A number of convective parameterization schemes have been developed over the years,

Description of the selected cumulus scheme

The Kain-Fritsch scheme is a mass flux scheme that uses downdraft and convective available potential energy (CAPE) removal time scales and includes cloud, rain, ice, and snow detrainment and cloud persistence over convective time scales. The scheme can account for the small-scale processes that lead to the development of convection (Kain et al., 1990).

Betts-Miller-Janji'c is an adjustment-type scheme that has deep and shallow profiles. It has no explicit updraft or downdraft and no cloud damage (Betts et al., 1992).

The Grell-Freitas scheme is a modification of the Grell-Devenyi ensemble scheme and is a multiclosure, multiparameter ensemble method with typically 144 subgrid members that tries to smooth the transition to cloud resolving scales. It has explicit updrafts and downdrafts and includes detrimental clouds and ice (Grell et al.,2014).

Description of Selected Microphysical Schemes

The SBU-YLin scheme includes ice, snow, and graupel processes and is suitable for real-time high-resolution simulations (Lin et al., 1983).

The WRF Single-Moment 6-class scheme includes ice, snow and graupel formation processes (Hong et al., 2006).

The New Thompson et al. scheme includes ice, snow, and graupel processes suitable for high-resolution simulations; it also adds rain number concentration apart from the ice number calculations performed in the model (Thompson et al., 2008).

For our case study, we used 9 schema combinations based on the intrinsic behavior of the atmosphere and chemical component modeling, as well as the thickness of the clouds modeled in the schemes. The associated combinations are shown in Table 2.

Table 2: Sensitivity experiments using different physical parameterizations: CU is the cumulus scheme, and MP is the microphysical scheme

Combination	MP	Reference	CU	Reference
KL	13	(Lin et al., 1983)	1	(Kain-Fritsch, 2000)
KW	6	(Hong et al., 2006)	1	(Kain-Fritsch, 2000)
KN	8	(New Thompson et al., 2009)	1	(Kain-Fritsch, 2000)
BW	6	(Hong et al., 2006)	2	(Betts-Miller-Janjic, 2002)
BL	13	(Lin et al., 2011)	2	(Betts-Miller-Janjic, 2002)
BT	8	(New Thompson et al., 2009)	2	(Betts-Miller-Janjic, 2002)
GT	8	(New Thompson et al., 2009)	3	(Grell-Freitas, 2013)
GL	13	(Lin et al., 2011)	3	(Grell-Freitas, 2013)
GF	6	(Hong et al., 2006)	3	(Grell-Freitas, 2013)

Table 2 shows the 9 combinations used in his references. The MP and CU columns present the code of the scheme in the namelist of the model, and the column of combinations has been established to facilitate naming.

Validation Methods

In statistics, a contingency table provides a basic picture of how two variables relate to each other and helps to identify interactions between them (Pearson et al., 1904). In atmospheric science, the contingency table is one of the most commonly used methods for dichotomous categorical verification of forecasts (Wilks et al., 1995). The data sets were counted into a 2 × 2 contingency table 3, with four elements from YY to NN based on whether an event was observed (YES/NO) and predicted (YES/NO).

Table 3: Contingency table for a dichotomous categorical verification of forecasts.

Forecast	Observed Yes	No	Total
Yes	Hits (a)	False alarms (b)	Forecast yes
No	Misses (c)	Correct rejection (d)	Forecast no
Total	observed yes	observed no	

We employed various statistical evaluations of precipitation indices, such as the accuracy, frequency bias, probability of detection, false alarm ratio and critical success index. These statistical methods are widely used in data analysis, and the contingency table is useful for assessing the prediction skill of the various indices and for finding appropriate thresholds provided by the categorical verification. The formulations of the aforementioned statistical skill scores are summarized in Table 4.

Table 4: Summary of statistical skill scores for evaluating the performance of the different configurations

Variable	Evaluation Method	Formula	Range	Perfect Score
	Accuracy	$PC = \frac{a+d}{N}$	0~100%	100%
	Frequency BIAS	$B = \frac{a+b}{a+c}$	0~∞	1
Rainfall occurrence	Probability of detection (POD)	$POD = \frac{a}{a+c}$	0~1	1
	False alarm ratio (FAR)	$FAR = \frac{b}{b+d}$	0~1	0
	Critical success index (TS)	$TS = \frac{a}{a+b+c}$	0~1	1

We can summarize all the stages of our work in the diagram below.
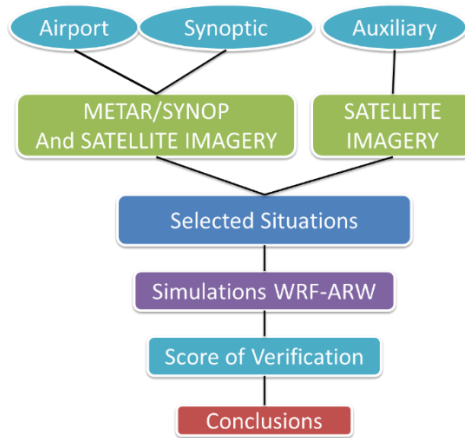
Figure 4: The steps followed

The work steps in Fig. 4 can be summarized as follows:

- The choice of data: the choice was made with caution. We started with the cumulation of precipitation during the chosen period of all the stations available on Eastern Algeria (Airport: Professional station for meta-aeronautical measurements with professional staff, Synoptic: Professional station for meteorological measurements with professional staff, Auxiliary: Professional station for meteorological measurements without staff).

- To validate the existence of a thunderstorm, METAR and SYNOP messages were examined as well as satellite images for airports and synoptic stations. However, for auxiliary stations, where there is no broadcast of messages, we have relied on satellite images of the company Eumetsat, particularly the RAPIDLY DEVELOPING THUNDERSTORM (RDT) product.

- After selecting and filtering the situations, only accumulations greater than 15 mm were collected as baseline observation data. Then, we simulate each situation using the combinations selected with the WRF model. To extract the data, a 12 km radius of interest around each station was applied.

- The simulation results were discussed with specific scores for validation, and conclusions were drawn.

RESULTS AND DISCUSSION

In this study, a threshold of verification was established:

-15 mm (BMS threshold): to check the quality of predictions for events that are the subject of the ONM Special Weather Report (BMS).

We collected the projected maximum precipitation at the grid points near the station within a 12 km radius. A tolerance radius was therefore applied around the station, as illustrated in Fig. 5.
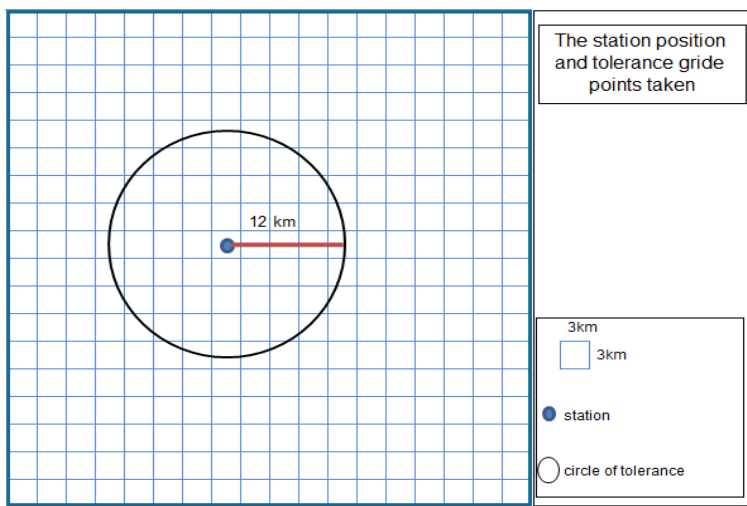
Figure 5: Station position and grid points considered for verification

Contingency table

The results of the contingency table are shown below in Table 5.

Table 5: Contingency table of forecast resaults

Observed Forecast		Yes			No		Total
Yes	KL = 4	BW = 0	GT = 2	KL = 0	BW =0	GT = 0	
	KW = 4	BL = 0	GL = 1	KW =0	BL = 0	GL = 0	18
	KN = 4	BT = 0	GF= 2	KN = 0	BT = 1	GF = 0	
No	KL = 12	BW=16	GT=14	KL = 0	BW= 0	GT = 0	
	KW =12	BL= 16	GL=15	KW= 0	BL = 0	GL = 0	126
	KN = 12	BT= 16	GF=14	KN = 0	BT = 0	GF = 0	
Total		143			1		144

The primary analysis of the contingency table reveals the superiority of the KL, KW, and KN combinations over all others. These combinations have shown outstanding performance and have emerged as the most successful ones.

On the other hand, the GT, GL, and GF combinations exhibited comparatively less success. While they may not be as effective as the top-performing combinations, they still show some degree of performance.

Finally, the BT, BL, and BW combinations were found to be the least successful among all the combinations. However, it is worth noting that they still exhibit decent performance, albeit not as impressive as the KL, KW, and KN combinations.

Skill Score Validation

The results of the validation scores are listed below in the table:

Table 6: The validation score results

Score	Combs								
	KL	KW	KN	BW	BL	BT	GT	GL	GF
Accuracy	25	25	5	0	0	0	12.5	6	12.5
BIAS	0.33	0.33	0.33	0	0	0.06	0.125	0.06	0.125
POD	0.25	0.25	0.25	0	0	0	0.125	0.06	0.125
FAR	0	0	0	0	0	1	0	0	0
TS	0.25	0.25	0.25	0	0	0	0.125	0.0625	0.125

The table displays the validation scores of nine combinations, and the following key observations can be made:

It is evident that combinations KL, KW, and KN exhibit identical and superior accuracy compared to the others with 25% accuracy. However, Grell Freitas's scheme combinations rank second in accuracy, albeit with a slightly lower score. Interestingly, the remaining combinations demonstrate zero accuracies, indicating their inability to capture the desired outcomes effectively.

BIAS: The analysis reveals a close relationship between bias and accuracy. Combinations KL, KW, and KN showcase the lowest bias values, indicating their ability to provide more balanced and accurate results. On the other hand, combinations GF and GT display higher bias compared to the top three combinations. The GL combination ranks third in terms of bias, while the other combinations exhibit even higher levels of bias.

Probability of Detection (POD): Combinations KL, KW, and KN stand out as the most sensitive among all combinations, indicating their high capability to detect the events of

interest. Conversely, combinations of GF and GT demonstrate lower efficiency in detection. The GL combination ranks third in terms of detection probability, while the other combinations fail to register any detection probability.

False Alarm Rate (FAR): The analysis indicates that only the BT combination triggers false alerts, suggesting that it produces a higher number of false alarms compared to the other combinations.

Threat Score (TS): Combinations KL, KW, and KN achieve the highest threat scores, indicating their strong performance in accurately capturing and predicting the desired events. However, combinations GT and GF attain the same TS values, but they exhibit lower overall skill. The GL combination ranks third in terms of threat score, while combinations BW, BL, and BT occupy the lower positions in the ranking.

In summary, the analysis reveals the superior accuracy and lower bias of the KL, KW, and KN combinations compared to the other combinations. Additionally, the analysis emphasizes the high sensitivity and detection probability of the KL, KW, and KN combinations. Finally, it underscores the strong threat score performance of combinations KL, KW, and KN. Consequently, it can be concluded that Kain Fritsch's scheme is the most effective. We may establish a principal connection that the new downdraft formulation in the KF scheme takes an approach in which key downdraft levels are linked specifically to the updraft, which is the major element that reinforces the intensity of rain in convective clouds (John et al., 2004). For example, precipitation-driven downdrafts that penetrate into the subcloud layer appear to originate just a few kilometers above the cloud base in more intense midlatitude convection over land (Knupp, 1987).

Grell Freitas's scheme, in particular, is the only one modified by microphysics. The Grell-Freitas scheme was primarily designed for global coarse cell models where convection depends on multiple parameters. Consequently, its sensitivity to microphysics and its limitations with a 3 km grid resolution can be justified (Zhang et al., 2003).

On the other hand, only the BT combination emits a false alarm. We can link this to the fact that the BMJ scheme assumes spatial homogeneity in the model grid cells, which may not accurately capture localized convective processes or small-scale variability (Fonseca et al., 2015).

CONCLUSION

To investigate the effects of physical schemes in the WRF-ARW model on heavy rainfall forecasting for the East Algerian area, 9 different model configurations were established by switching three typical cumulus parameterization schemes and three cloud microphysics schemes from simple to complex schemes. The 144 experiments of widespread heavy rainfall occurring in the study area used boundaries from the GFS model and had a horizontal resolution of 3 km × 3 km.

Based on the assessments conducted, the main conclusion drawn is that the Kain-Fritsch cumulus scheme (KF) outperformed the other schemes in terms of overall performance. This superiority can be attributed primarily to the scheme's consideration of the effect of ascendance, which acts as the driving force behind isolated convections in the middle latitudes. This observation aligns with the findings previously put forth by (John et al., 2004), further establishing the effectiveness of the Kain-Fritsch scheme specifically in the middle latitudes.

On the other hand, the microphysical effect is only evident in the Grell Freitas scheme. This can be attributed to the scheme's intrinsic characteristics, as it takes into account numerous variables in the treatment of convections. Consequently, this scheme is more likely to trigger thunderstorms with heavy rainfall in global models, as highlighted in the study conducted by Zhang et al. (2003).

It is crucial to acknowledge that the impact of different physical parameters plays a decisive role in the simulation of extreme precipitation events. These parameters significantly influence the accuracy and representation of such events in the models used for simulations.

A key point that can be addressed in future research is to arrange the adjustable parameters in its schemes that can give more precision and effectiveness.

However, we did not address the quality of the couplers, boundary conditions, and other physical schemes in our research, as they are considered less efficient. Nonetheless, they still pose a potential source of errors that should not be overlooked.

It is important to note that the specific behavior of WRF configurations with degraded scores can vary based on the factors being evaluated, the specific model setup des schemes, the region being simulated, the initial and boundary conditions, and the specific phenomena evaluated.

Declaration of competing interest

The authors declare that they have no known competing financial interests or personal relationships that could have appeared to influence the work reported in this paper.

REFERENCES

ALAN A. (2007). An Introduction to Categorical Data Analysis, Second Edition, Department of Statistics, University of Florida, Gainesville, Florida, 394p.

CHERKI K. (2019). Daily and instantaneous flood forecasting using artificial neural networks in a north–west Algerian watershed, Larhyss Journal, No 40, pp. 27-43.

CURTIS R. ALEXANDER, JORDAN G. POWERS, JOSEPH B, KLEMP, WILLIAM C, SKAMAROCK, CHRISTOPHER A, DAVIS, JIMY D, DAVID O, GILL, JANICE L. COEN, DAVID J, GOCHIS, RAVAN A, STEVEN E. PECKHAM, GEORG A.

GRELL, JOHN M, SAMUEL T, STANLEY G. BENJAMIN, GEOFFREY J. DIMEGO, WEI W, CRAIG S. SCHWARTZ, GLEN S. ROMINE, ZHIQUAN L, CHRIS S, FEI C, MICHAEL J. BARLAGE, WEI Y, MICHAEL G. DUDA. (2017). The Weather Research and Forecasting Model: Overview, System Efforts, and Future Directions. Bulletin of the American Meteorological Society, 22 p.

BETTS A.K., MILLER M.J., JANJIC Z.I. (1992). Betts-Miller-Janjic cumulus parameterization in the NCEP Eta Model, NCEP Office, Vol. 397, pp. 107-121.

BONG C.H.J., LIEW S.C., SIM J.E., TEO F.Y. (2023). Trend and statistical analysis of annual maximum daily rainfall (AMDR) for Sarawak river basin, Sarawak, Malaysia, Larhyss Journal, No 53, pp. 183-197.

FONSECA R.M., MORALES C.A., FISCH G., CHOU S.C. (2015). Sensitivity of WRF-ARW simulated mesoscale convective system rainfall to the choice of parameterization schemes. Atmospheric Research, Vol. 158, pp. 145-159.

GRELL G.A., FREITAS S.R. (2014). A Scale- and Aerosol-Aware Stochastic Convective Parameterization for Weather and Air Quality Models, Atmospheric Chemistry and Physics, Vol. 14, Issue 10, pp. 5233-5250.

HIREN S.L., RANJAN K.J. (2018). Analysis of Extreme Rainfall Event with Different Microphysics and Parameterization Schemes in WRF Model, Scientific Research, Vol. 9, Issue 1.

HAFNAOUI M.A., MADI M., BEN SAID M., BENMALEK A. (2022). Floods in El Bayadh city: causes and factors, Larhyss Journal, No 51, pp. 97-113.

HONG S.Y, LIM J.O.J. (2006). The WRF Single-Moment 6-Class Microphysics Scheme (WSM6), Journal of the Korean Meteorological Society, Vol. 42, Issue 2, pp. 129-151.

JORGE J.S.B., IGOR G. (2022). Impact of Cumulus Parameterizations on the Simulation of a Torrential Rainfall Event over the Southeast of the Iberian Peninsula, Social Science Research Network, pp.31.

JULIA J., GREGORY W., ROLAND S. (2019). Evaluation of Cumulus and Microphysics Parameterizations in WRF across the Convective Gray Zone, Weather and Forecasting, Vol. 34, Issue 4, pp. 1097-1115.

KAIN J.S., FRITSCH J.M.A. (1990). One-Dimensional Entraining Detraining Plume Model and Its Application in Convective Parameterization, Journal of the Atmospheric Sciences, Vol. 47, Issue 23, pp. 2784-2802.

KAIN J.S. (2004). The Kain–Fritsch convective parameterization: an update, Journal of Applied Meteorology, Vol. 43, pp. 170-181.

KNUPP K.R., (1987). Downdrafts within High Plains cumulonimbi. Part I: General kinematic structure, Vol. 44, Issue 6, pp. 987-1008.

LIN Y., FARLEY R.D., ORVILLE H.D. (1983). Bulk Parameterization of the Snow Field in a Cloud Model, Journal of Climate and Applied Meteorology, Vol. 22, Issue 6, pp. 1065-1092.

NASSA R.A.K., KOUASSI A M., BOSSA S.J. (2021). Analysis of climate change impact on the statistical adjustment models of extreme rainfall case of Ivory Coast, Larhyss Journal, No 46, pp. 21-48.

PANG J.M., TAN K.W. (2023). Development of regional climate model (rcm) for Cameron highlands based on representative concentration pathways (rcp) 4.5 and 8.5, Larhyss Journal, No 54, pp. 55-70.

SKAMAROCK W.C., KLEMP J.B., DUDHIA J., GILL D.O., BARKER D.M., WANG W., POWERS J.G. (2008). A description of the advanced research WRF version 3, NCAR Technical Note NCAR/TN-475+STR. National Center for Atmospheric Research, Boulder, Colorado, USA, 113 p.

THOMPSON G., FIELD P.R., RASMUSSEN R.M., HALL W.D. (2008). Explicit Forecasts of Winter Precipitation Using an Improved Bulk Microphysics Scheme, Part II: Implementation of a New Snow Parameterization, Monthly Weather Review, Vol. 136, Issue 12, pp. 5095-5115.

TIEN D.D., CUONG H.D., LARS R.H., LAM H., HUYEN L.T.T., HUNG M.K. (2019). Impacts of Different Physical Parameterization Configurations on Widespread Heavy Rain Forecast over the Northern Area of Vietnam in WRF-ARW Mode, Advances in Meteorology, Vol. 2019.

TRIPHONIA J.N., NYIMVUA S., JOACHIM R., MICHEL D.S., MESQUITA EDWIN R., ISAAC M., CHIKU S. (2018). Assessing Weather Research and Forecasting (WRF) Model Parameterization Schemes Skill to Simulate Extreme Rainfall Events over Dar es Salaam on 21 December 2011, Journal of Geoscience and Environment Protection, Vol. 6, Issue 1.

CHARLES A., DOSWELL I. (1993). Flash Flood-Producing Convective Storms: Current Understanding and Research. NOAA ERL National Severe Storms Laboratory Norman, Oklahoma USA, 10 p.

RODERICK L., ALAN L., SREEJA N., VINAY R. (2021). Prediction models for urban flood evolution for satellite remote sensing. Journal of Hydrology, Vol. 603, Part D, pp. 127-175.

TRIPHONIA A., MOHANTY U.C., PANIGRAHI A. (2018). Parameterization Schemes in Numerical Weather Prediction Models: A Review, Journal of Earth System Science, 68 p.

YANDY G.M., MICHEL D.S.M. (2015). Numerical Simulations of the 1 May 2012 Deep Convection Event over Cuba: Sensitivity to Cumulus and Microphysical Schemes in a High-Resolution Model, Hindawi: Advances in Meteorology, Vol. 2015.

YASMIN K. L. K., ERICK G.S.N., NOÈLE B.P.D.S., PEDRO Z.J., PRASHANT K., TACIANA T. D. A.A., MARCELO R.D.M., DAVIDSON M.M. (2022). Evaluation of the WRF-ARW model during an extreme rainfall event: Subtropical storm Guará, Atmósfera, Vol. 35, Issue 4.

ZEGGANE H., GHERNAOUT R., BOUTOUTAOU D., ABDULLAH S.S., REMINI B., KISI O. (2021). Multidimensional analyses of precipitation in Central-Northern region of Algeria, Larhyss Journal, Vol. 47, pp. 209-231.